SANDIA REPORT
SAND2008-6668
Unlimited Release
Printed December 2008

Neutral Atom Traps

Michael V. Pack

Prepared by
Sandia National Laboratories
Albuquerque, New Mexico 87185 and Livermore, California 94550

Sandia is a multiprogram laboratory operated by Sandia Corporation,
a Lockheed Martin Company, for the United States Department of Energy's
National Nuclear Security Administration under Contract DE-AC04-94AL85000.

Sandia National Laboratories

Issued by Sandia National Laboratories, operated for the United States Department of Energy by Sandia Corporation.

NOTICE: This report was prepared as an account of work sponsored by an agency of the United States Government. Neither the United States Government, nor any agency thereof, nor any of their employees, nor any of their contractors, subcontractors, or their employees, make any warranty, express or implied, or assume any legal liability or responsibility for the accuracy, completeness, or usefulness of any information, apparatus, product, or process disclosed, or represent that its use would not infringe privately owned rights. Reference herein to any specific commercial product, process, or service by trade name, trademark, manufacturer, or otherwise, does not necessarily constitute or imply its endorsement, recommendation, or favoring by the United States Government, any agency thereof, or any of their contractors or subcontractors. The views and opinions expressed herein do not necessarily state or reflect those of the United States Government, any agency thereof, or any of their contractors.

SAND2008-6668
Unlimited Release
Printed December 2008

Neutral Atom Traps

Michael Pack Org. 1128

Sandia National Laboratories
P.O. Box 5800
Albuquerque, New Mexico 87185-MS1415

Abstract

This report describes progress in designing a neutral atom trap capable of trapping sub millikelvin atom in a magnetic trap and shuttling the atoms across the atom chip from a collection area to an optical cavity. The numerical simulation and atom chip design are discussed. Also, discussed are preliminary calculations of quantum noise sources in Kerr nonlinear optics measurements based on electromagnetically induced transparency. These types of measurements may be important for quantum nondemolition measurements at the few photon limit.

INTRODUCTION

This report describes progress in two areas of atomic physics; neutral atom traps, and noise sources in nonlinear optics based on electromagnetically induced transparency (EIT). Our emphasis is to develop the necessary tools and understanding required for quantum nondemolition (QND) measurements of photon number. The goal is to increase the resolution of the QND measurements until it is possible to resolve individual photons, and it seems the best path to single-photon resolution is via the giant Kerr optical nonlinearities provided by EIT.

The development of magnetic neutral atom traps is important because it provides a small, dense cloud of atoms in a single velocity class as the EIT medium. Also, atom traps can be used to move the atoms from a collection region into an optical cavity where the coupling between atoms and photons becomes even stronger.

There are also some fundamental problems which need to be better understood in order to determine what the fundamental limits are on signal to noise ratio for QND measurements. Over the past 20 years numerous proposal have been advanced which rely on Kerr nonlinearities to realize quantum computing or quantum information tasks. Recent research has looked at how fundamental noise limits set bounds on the fidelity for two-qubit gates based on Kerr nonlinearities. This research has raised doubts whether early research adequately accounted for all the noise sources affecting the Kerr QND measurements.

1 — ATOM CHIP DESIGN

Neutral atom chips have generated tremendous interest in the field of cold atom physics because the offer greater control, lower currents, and decrease the challenges in atomic cooling and trapping experiments. At Sandia our interest has been in applying our technical expertise in microfabrication to improve upon the atom chip success at numerous universities, and to develop the ability to tap atoms and move them into an optical cavity for cavity QED experiments. In this report we discuss an atom chip design we have developed to collect and trap alkali atoms in a magneto-optical trap (MOT). Our atom chip then transfers the atoms from the MOT to a smaller magnetic trap, which is used to transport the atoms 7 mm across the atom trap surface to an optical cavity.

The organization of our atom chip discussion is divided into three parts. First, we discuss the numerical techniques developed to calculate the magnetic fields for designing an simulating the magnetic chip traps. Second, we present the design of the atom chip. Finally, we discuss the numerical simulation tools for calculating loss and heating due to atom transportation across the chip. At the time of this report we have not obtained sufficient results from the heating simulations to report on them.

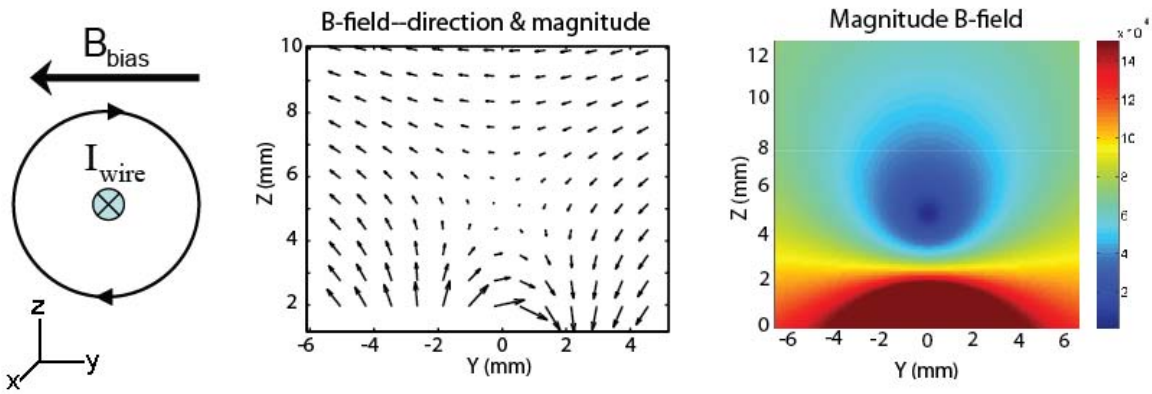

Figure 1.1: A simple side guide 2D magnetic trap. The magnetic field from a wire cancels with a uniform bias field along onside of the wire creating a quadrupoles magnetic trap for paramagnetic atoms.

1.1 — Magnetic field calculations for atom chips

Magnetic traps of neutral atoms use the coupling between an atoms magnetic dipole moment and an external B-field to create a potential well deep enough to confine the motion of low temperature atoms. Practical limitations (e.g. maximum electical currents, atomic dipole moments, etc.) limit the trappable atom temperature to the sub-millikelvin range.

In order to understand our choice of method in solving for magnetic fields, it is helpful to give a rough definition of the problem. Figure 1.1 shows the simplest magnetic trap for atoms. A wire is centered at the origin and runs along the x-axis with electrical current in the negative x direction. An external bias magnetic field is directed along the negative y direction. In the *yz* plane the combination of the B-field from the wire and the bias field creates a null at a distance

$$y = \frac{\mu_0 I_{wire}}{2\pi B_{bias}} \tag{1.1}$$

above the wire. This is quadrupole waveguide for paramagnetic atoms, because it will only confine the atoms in two dimensions. Additional wires and B-fields can create confinement in the z-dimension.

The energy potential for an alkali atom in an inhomogeneous magnetic field on is given by

$$\Delta E_{|F\, m_F\rangle} = \mu_B g_F m_F B_z, \tag{1.2}$$

where μ_B is the Bohr magneton, m_F is the electron spin for a given magnetic hyperfine sublevels, B_z is the magnetic field which is assumed to be entirely along the quantization axis, and hyperfine Landé *g*-factor is given by

$$g_F = g_J \frac{F(F+1) - I(I+1) + J(J+1)}{2F(F+1)} + g_I \frac{F(F+1) + I(I+1) - J(J+1)}{2F(F+1)}, \tag{1.3}$$

where $J = L + S$ is the total electron angular momentum (*L* is the electron orbital angular momentum and *S* is the electron spin angular momentum) and $F = J + I$ is the total atomic angular momentum (*I* is the total nuclear angular momentum).

Using optical pumping with circularly polarized light it is straightforward to align the spins in a cloud of cold alkali atoms such that they are all in the stretched state $\left|F, m_F = F\right\rangle$, in which case the energy potential is the deepest. If the atoms are in an inhomogeneous magnetic field with spatial varying directionality, the atoms internal state tends to adiabatically follow the field such that is the start in the stretched state they will stay in the stretched state. Thus, in designing a magnetic microtrap for neutral atoms one needs only to consider the magnitude of the magnetic field, and initial preparation of the magnetic states. If the atoms become extremely cold (e.g. in evaporative cooling to create a BEC) there is an increased likelihood of Majorana spin flips as the atoms pass through a region of near zero magnetic field because there is no clear quantization axis in these regions. In this case an Ioffe-Pritchard trap is preferable, but we will not discuss the case extremely cold atoms further in this report.

We solve the problem of finding the magnetic fields due to a current carrying wire of arbitrary shape by dividing the wire up into many sections of straight wires with different lengths and direction, which added together equal the arbitrary wire shape. It is well known that that the B-field at position $\boldsymbol{r}$ due to current I_{wire} flowing along straight wire from point $\boldsymbol{r_1}$ to $\boldsymbol{r_2}$ is given by

$$\mathbf{B} = \frac{(\boldsymbol{r}\text{-}\boldsymbol{r_1})\times(\boldsymbol{r_2}\text{-}\boldsymbol{r_1})}{\|(\boldsymbol{r}\text{-}\boldsymbol{r_1})\times(\boldsymbol{r_2}\text{-}\boldsymbol{r_1})\|}\frac{\mu_0 I_{wire}}{4\pi d}(\sin\theta_2 - \sin\theta_1), \qquad (1.4)$$

where $\sin\theta_i = (\boldsymbol{r}\text{-}\boldsymbol{r_i})\cdot(\boldsymbol{r_2}\text{-}\boldsymbol{r_1})/\|\boldsymbol{r}\text{-}\boldsymbol{r_i}\|\,\|\boldsymbol{r_2}\text{-}\boldsymbol{r_1}\|$ and $d = \|\boldsymbol{r}\text{-}\boldsymbol{r_i}\|\cos\theta_i$. When a wire cannot be assumed to be infinitely thin we assume that the current is evenly distributed across the cross section of the wire and approximate the large wire by several infinitesimal wires distributed through out the cross section. To choose the positions and weighting (i.e. current distribution) of the sub-wires we use Gauss-Legendre Quadrature integration.

The first step in almost all cold atom experiments is the cooling and trapping of atoms in a MOT. On an atom chip this can be done with a mirror MOT where the surface of the atom chip is a mirror. Figure 1.2 shows a diagram from Dana Anderson's research group describing the operation of a mirror-MOT. In a typical MOT without the atom chip anti-helemholtz coils create a quadrupole magnetic field and six circularly polarized laser fields provided Doppler cooling. In the mirror MOT two of the laser beams are replaced by reflections off of the mirror surface, and the experiment can be further simplified by replacing the anit-helmholtz coils with a macroscopic U-shaped wire next to the non-mirror surface of the atom chip. As seen in Fig. 1.1 a wire in a bias field results in a quadrupole magnetic field similar to the anti-helmholtz coils. However, the wires which can be fabricated on an atom chip are much to small to care the current necessary for realizing a MOT with sufficiently large capture volume to cool and trap room temperature atoms.

To obtain a large capture volume a macroscopic sized U-trap must be used. Figure 1.3 shows several views of the macro U (yellow) and atom chip (blue) being used in current experiments at Sandia. The macro U is an anodized copper wire with a rectangular cross section of 2.5 mm by 5mm, and the length of the bottom and sides of the U are 12 mm and 34 mm respectively. The current through the U is about 30 A, and the bias field is maintained near 10 Gauss. Figure 1.4 shows calculations the magnetic fields using Matlab®. Surface of constant magnetic field are plotted using different colors. Obviously with how close the magnetic field null is to the wires and the size of the wires it would not be realistic to model the macro U as a single infinitesimally thin wire. These simulations are important both for the initial design of the experimental apparatus, and also as a guide aligning and optimizing the MOT for evolving experiments.

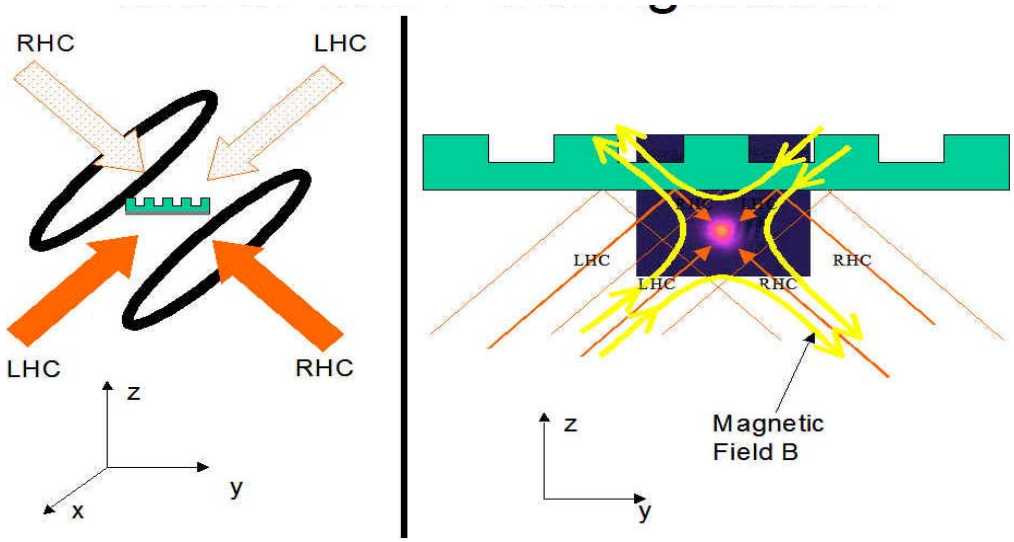

Figure 1.2: Circularly polairazed laser beams are preferentially absorbed by Doppler shifted atomic transitions in atoms moving anti-parallel to the laser direction of propagation. Quadrupole magnetic fields Zeeman shift the atoms such that the net force due to stimulated absorption of the lasers traps the atom at the magnetic null.

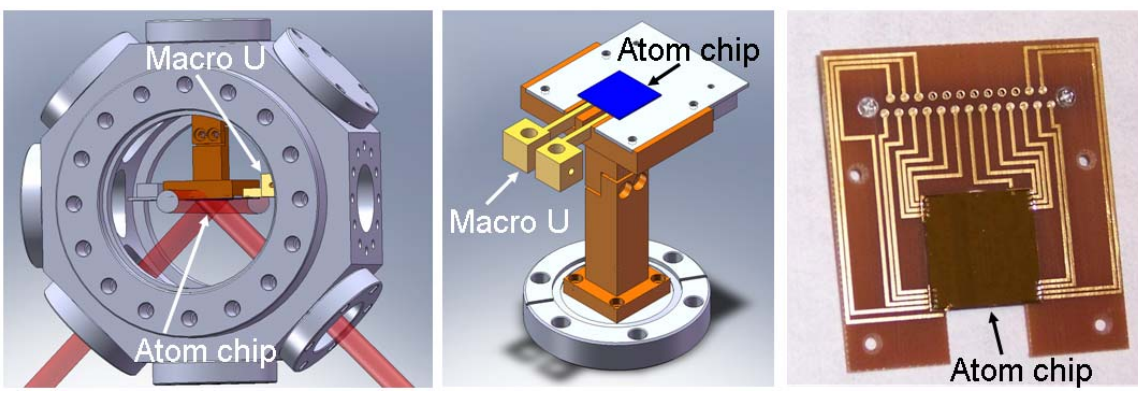

Figure 1.3: Solid works drawings by Kevin Fortier and picture of the atom chip being used in cold atom experiments at Sandia NM. and trapping in a MOT.

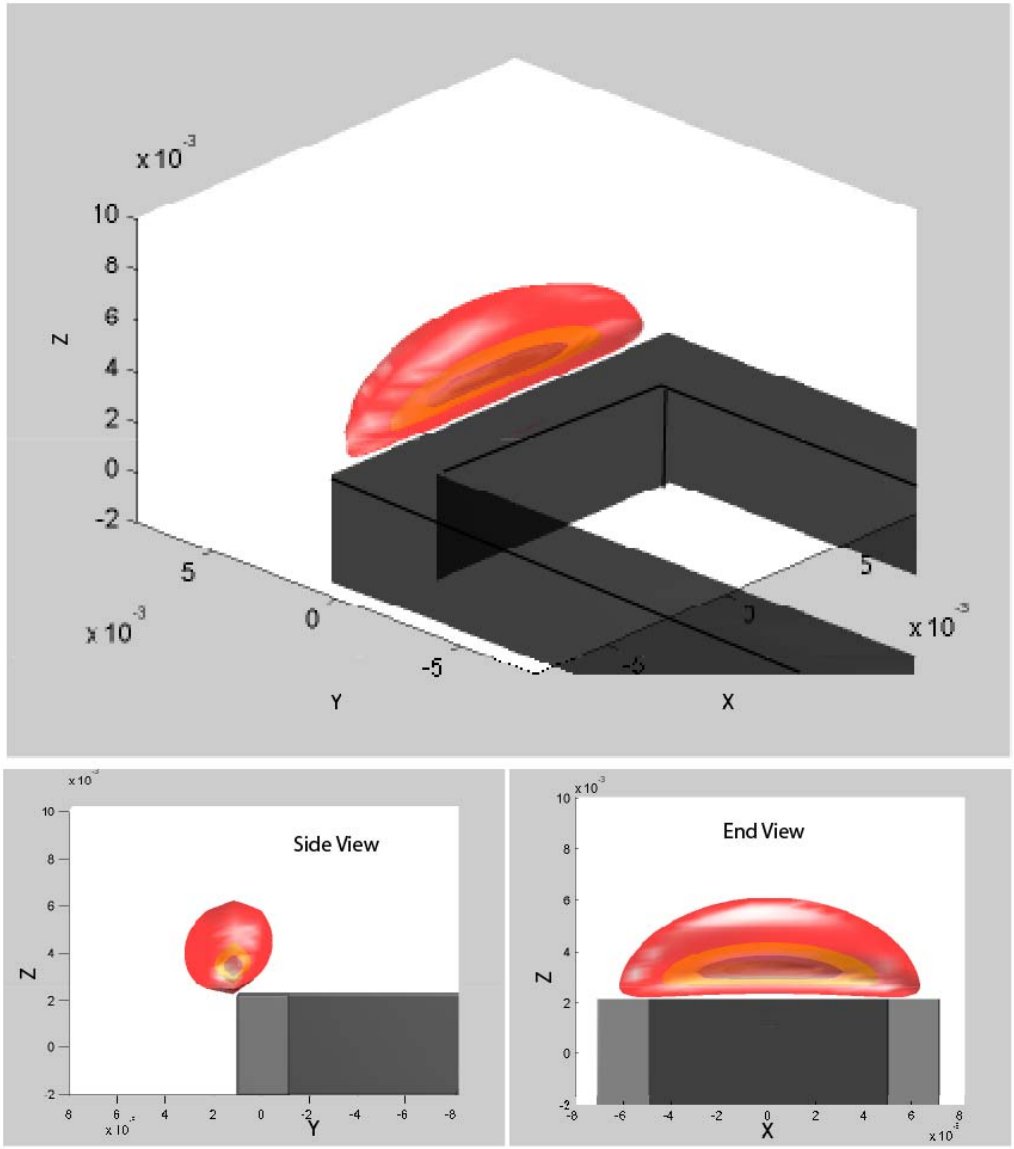

Figure 1.4: Numerical calculations of energy potential due to magnetic trapping of neutral atoms.

1.2—Atom Chip Design

The goal of the atom chip is to transfer atoms collected in the MOT to a purely magnetic trap and then transport them along the surface of the atom chip to an optical cavity. We adopt a similar approach to J. Reichel's research group for "long distance" transport of atoms[1]. We use a two metallization layer design with the top layer creating a magnetic waveguide similar to the waveguide shown in Fig, 1.1, and the bottom metallization layer providing a conveyor belt for precision control and movement of the atoms along the waveguide. The upper metallization layer is shown in Fig. 1.5, and it consists of three metal strips. The inner conductor (red) has a rather complicated shape because it is required to satisfy numerous functions as we will describe

shortly. The inner conductor has an outer conductor running along both sides to provide the bias field for the wave guide. There is also a lower metallization layer which is discussed later.

This atom chip is designed to move the atom cloud from the MOT to an optical cavity. There is also a compression of the atom cloud that occurs, but this is of secondary importance. To transfer atoms from the MOT to a magnetic trap, the current through the MOT macro U (shown in Figs. 1.3 and 1.4) is ramped down as the current in the P-shaped inner conductor (shown as black in Fig. 1.6) is ramped up. Figure 1.6 shows the direction of the bias magnetic field (which is on for both the MOT and the magnetic trap) and the direction of current flow through the P. The Bias field is provided by coils external to the vacuum chamber. After the atoms are completely transferred to the magnetic trap, the bias field is rotated to point in the positive *y* direction such that magnetic trap minimum rotates down to the top of the P.

Next the current in the P is ramped down while current through the Z trap is ramped up. The Z trap can be used for evaporative cooling to decrease the average atom temperature and decrease the atom cloud size. It is also a transitional trap to prepare and load the atom waveguide.

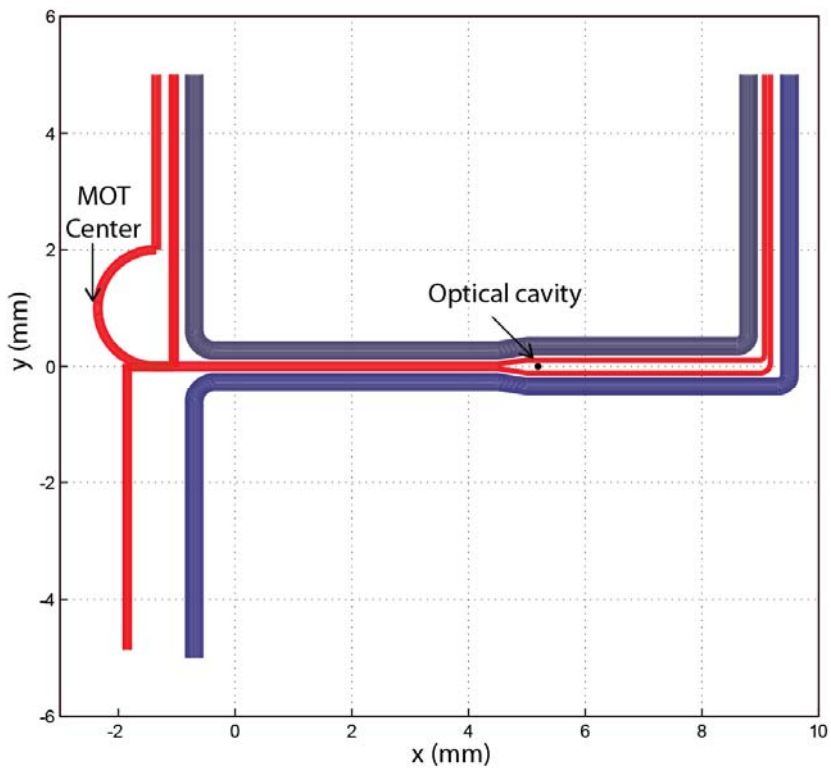

Figure 1.5: Upper metallization layer for atom chip design to move a cold atom cloud from the collection region (i.e. the MOT) to a micro optical cavity for cavity QED experiments.

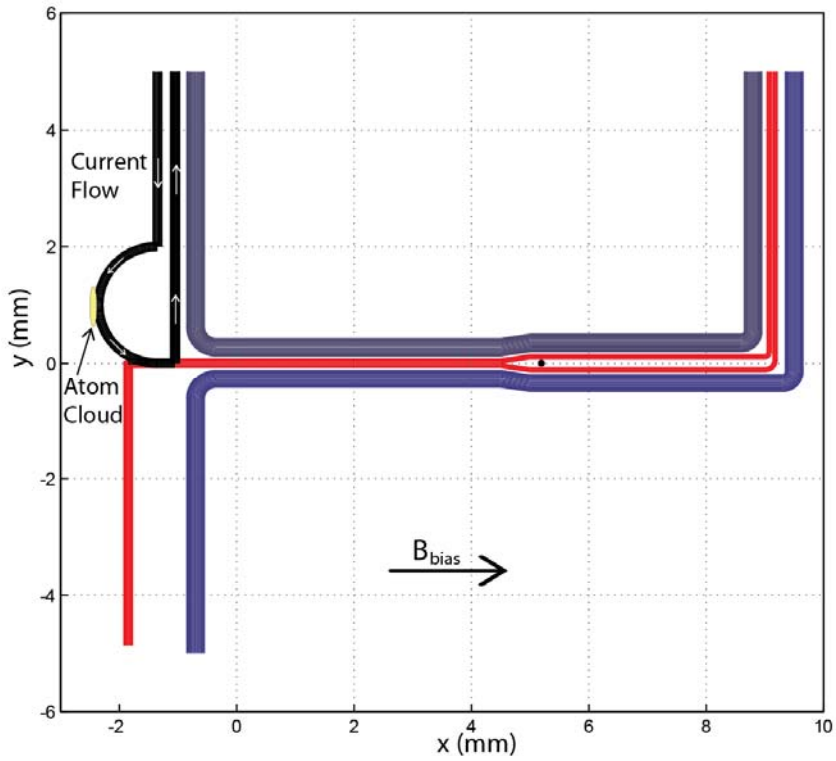

Figure 1.6: In the first part of the atom transport the atoms are transferred from the MOT to an optical trap by ramping down the MOT currents and ramping up the current in the P-shaped wire (black).

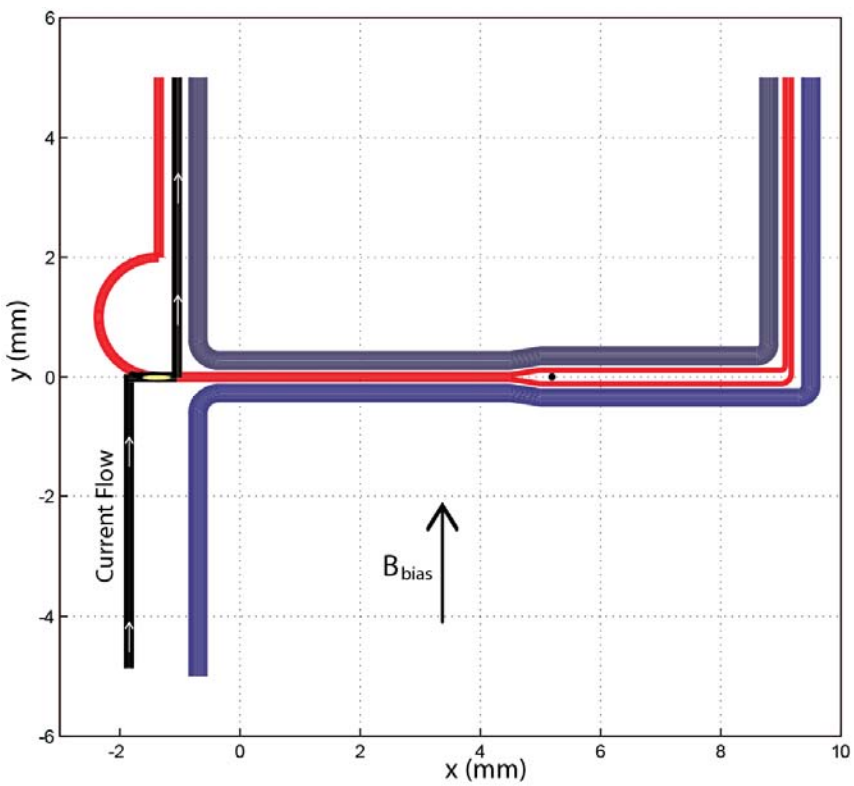

Figure 1.7: The atoms are moved towards the waveguide by rotating the bias field and transferring current from the P-trap to the Z-trap (black).

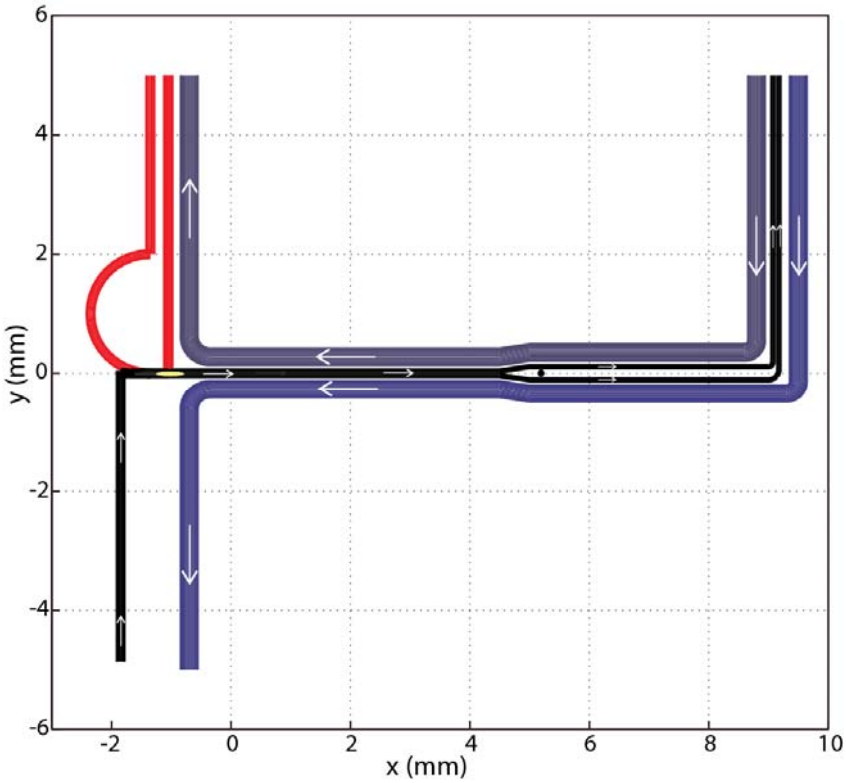

Figure 1.8: With the atoms in position current is redirected along the long waveguide. When the atoms have moved between the outer conductors (purple) the current in the outer conductors ramps up and the bias field ramps down.

As the currents and bias field transfer over to the waveguide configuration shown in Fig. 1.8, the confinement of the atoms along the *x* direction is provided by currents running through the lower layer of metallization. Also we note that once the atom cload has moved to a region in between the outer conductors, the bias field in the *y* direction can be turned off because the current through the outer conductors will provide this bias field. The advantage of using the outer conductors to create the bias field is that they consume less power than using a coil outside the chamber. They don't require alignment, and can turn on and off more quickly than external bias coils. Also the outer conductor provide additional flexibility because by using both the external bias coils and current through the outer conductor we can create a strong bias field and deeper magnetic trap than is possible with just one or the other.

Figure 1.9 shows how the lower metallization layer provides confinement in the x direction and how modulating the currents on this layers mover the magnetic trap and the atoms along the atom chip. In Fig. 1.9 only two wires (colored magenta and cyan) are shown on the lower metallization layer for simplicity, but in the actual atom chip there are six wires on the lower metallization layer as shown in Fig. 1.10. The wires with current flowing in the positive y direction add to the bias field creating a higher potential energy for the atoms and wires carrying current in the negative y direction cancel out the bias field to create the trap minimum. In a two wire configuration as shown in Fig. 1.9 the currents have a sinusoidal modulation with phase of the magenta wire leading the cyan wire by ninety degrees. By using more than two wires as

shown in Fig. 1.10 the magnetic trap can be walked down the wave guide more smoothly and more complex trap shapes and modulation schemes can be attempted.

When the atom cloud moves close to the center conductor bifurcates to go around the optical cavity. This serves two purposes. First, the metal layer cannot go into the optical cavity. Second, the split wire configuration provides precision control of the *z* dimension of the magnetic trap. Bringing the atoms into the optical cavity and optimization of the atom cloud position inside the optical cavity requires fine control over all dimensions of the magnetic trap. Two wires carrying equal and parallel currents create a magnetic minimum at a distance half way between them and this magnetic minimum can be moved above or below the plane of the wires by turning on a bias magnetic field perpendicular to the wires but parallel to the plane containing the wires. And this is precisely the strategy we have employed for controlling the height of the magnetic trap above the atom chip as the atoms are moved into the optical cavity.

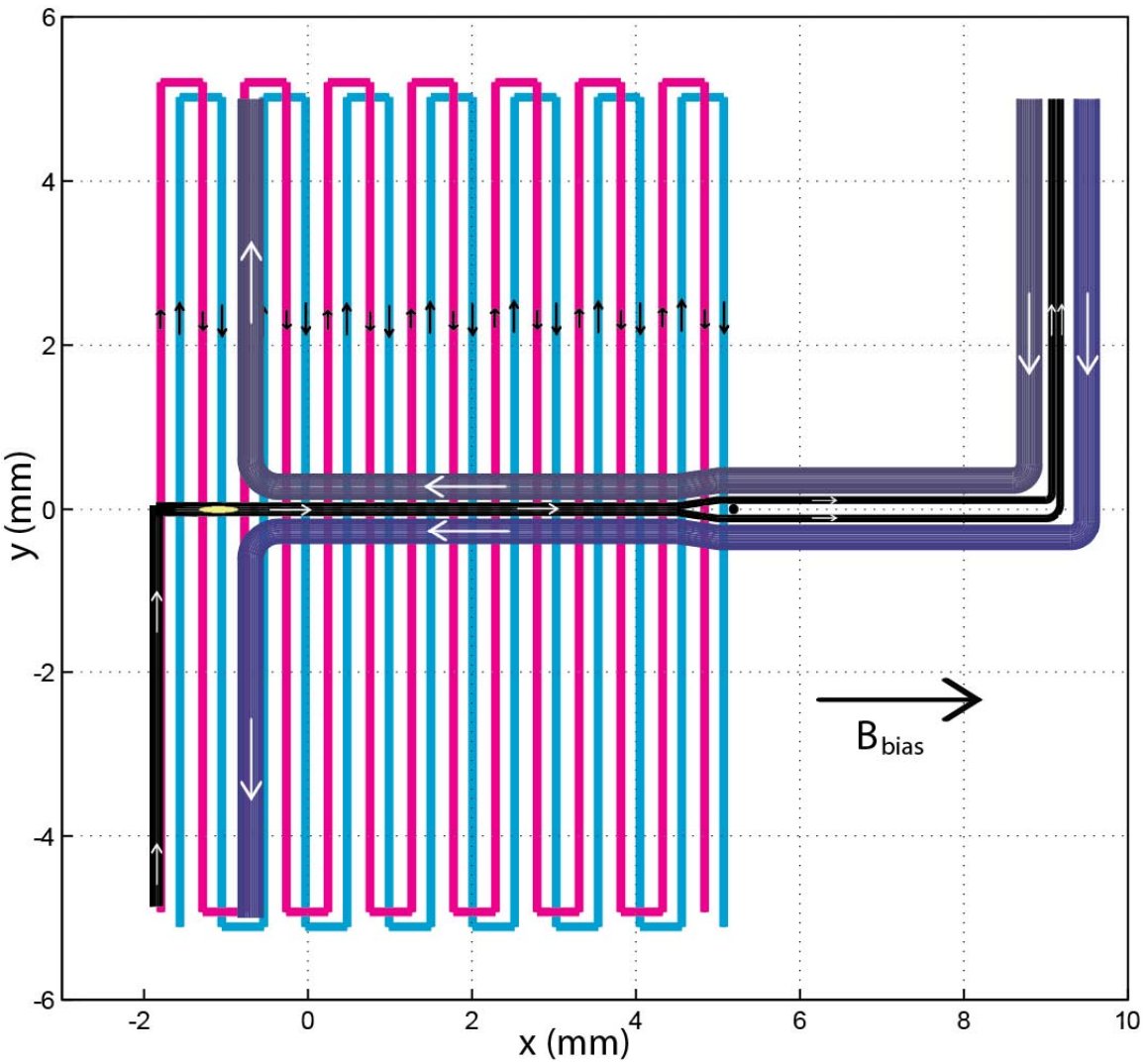

Figure 1.9: The lower metallization layer provides confinement of the atoms in the *x* direction by canceling out magnetic bias field in the positive *x* direction.

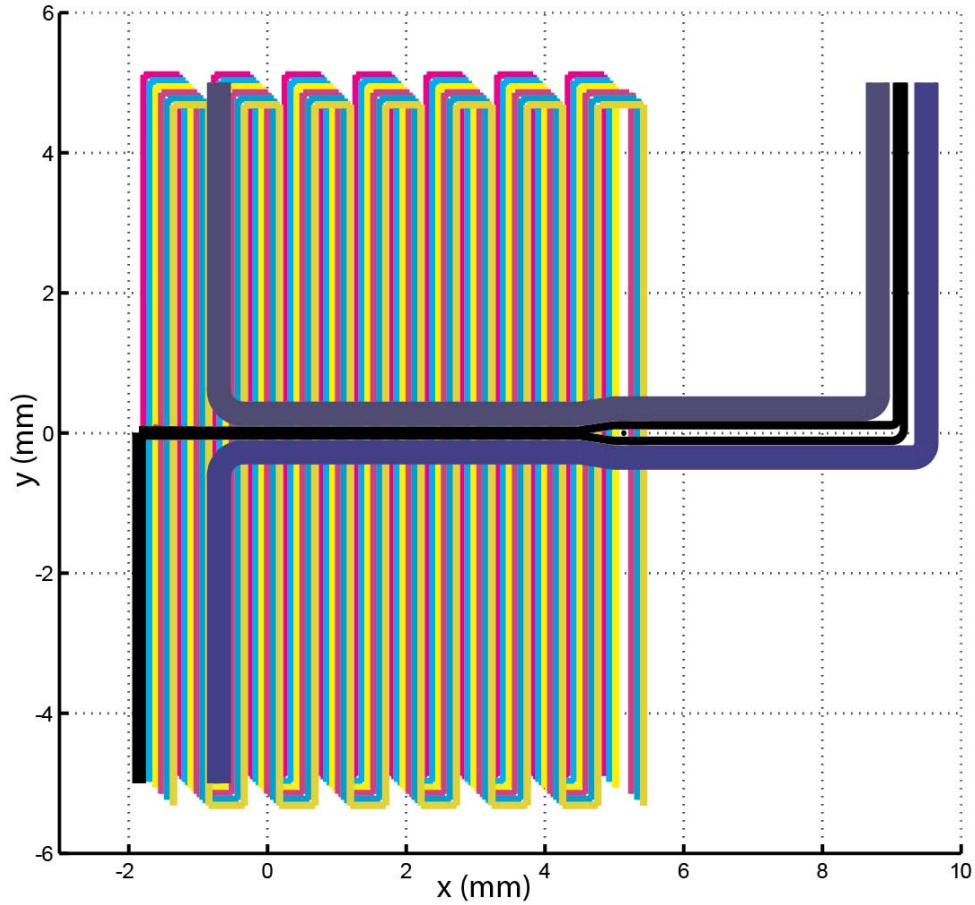

Figure 1.10: All metallization layers (without P-trap) each metal wire is a different color. All six lower metallization wires are shown.

We have also investigated other atom chip design such as the single layer conveyor.[2] This design uses sinusoidal modulation of the two side conductors with a 90 degree phase lag between the two currents to move a magnetic trap minimum along the Z-trap waveguide. Figure 1.11(a) shows each current carrying wire as a different color, and Fig. 1.11(b) shows the magnetic field when the current in one of the side conductors is at zero. In this design the magnetic minima wandered back and forth across the center wire with each current modulation cycle. It was thought that this movement would introduce unnecessary heating and thus it was abandoned.

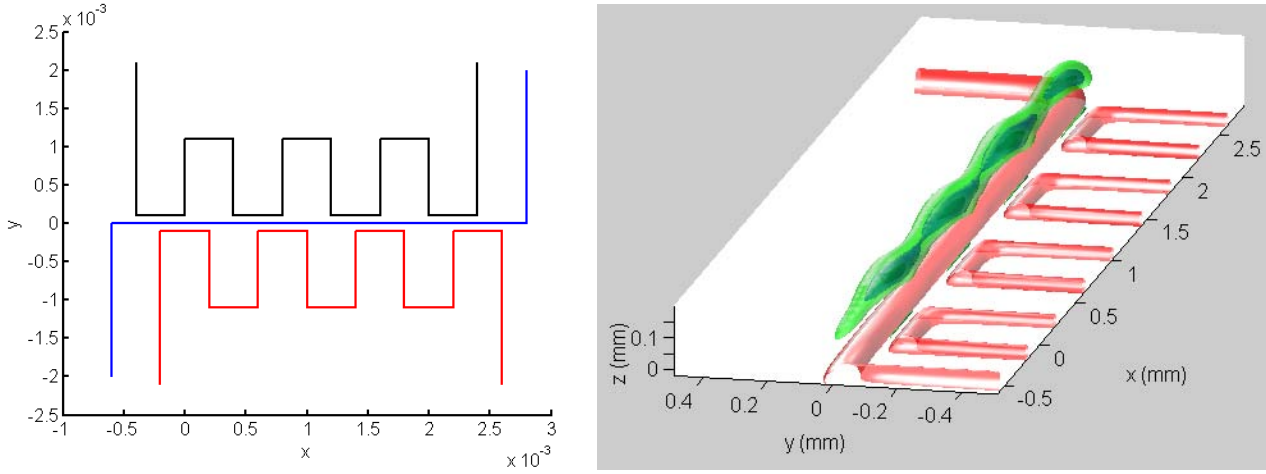

(a) (b)

Figure 1.11: Atom conveyor belt design for a single metallization layer (a), and simulation of the magnetic field strength (b).

1.3—Atom Heating and Loss

For an uncorrelated cloud of atoms, anytime you change the trap potential you should expect to heat the atoms, which will also increase atom loss from the trap. Of course, there will also be loss if you do nothing. The goal for the atom chip is to make all changes to the magnetic trap adiabatically in order to minimize heating and still move the atoms quickly because longer times mean greater ambient loss. The best solution gets the most atoms from the MOT to the optical cavity by balancing ambient loss which compounds over time with heating loss due to quick changes in the magnetic trap.

Unfortunately we have not yet solved for the optimal dynamics for the current that gets the most atoms to the optical cavity, but we have already developed the numerical tools to do this. The force of the magnetic trap on the atoms in given by taking the negative gradient of the enegy given by Eq. (1.2), i.e.

$$F = -\nabla U = -\mu_B g_F m_F \nabla B. \qquad (1.6)$$

Using the Runga-Kuta algorithms it is straightforward to integrate and obtain the atoms position as a function of time. Figure 1.12 shows the initial positions of a thermal atom cloud before a simulation of a Z-trap. No atom-atom interactions are considered in the simulations. Figure 1.13 shows the simulated trajectory of one of the atoms in the Z-trap. While we have not yet used these tools to determine the best operating regime for the atom chip, they are available to provide guidance once experiments commence.

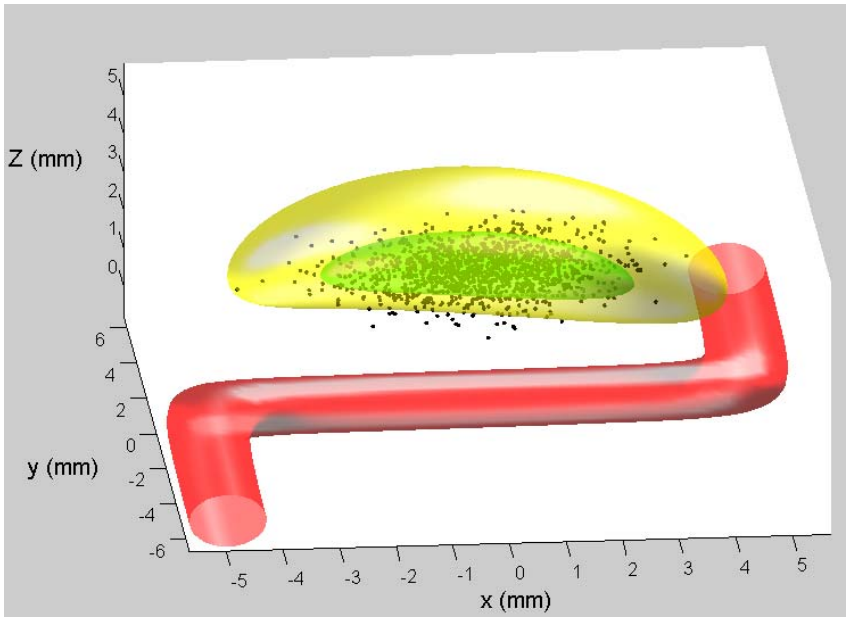

Figure 1.12: Initialization of the atom cloud. Each atom is randomly assigned a position according to the potential energy as a function of position and average atom temperature, and a momentum according to the average atom temperature.

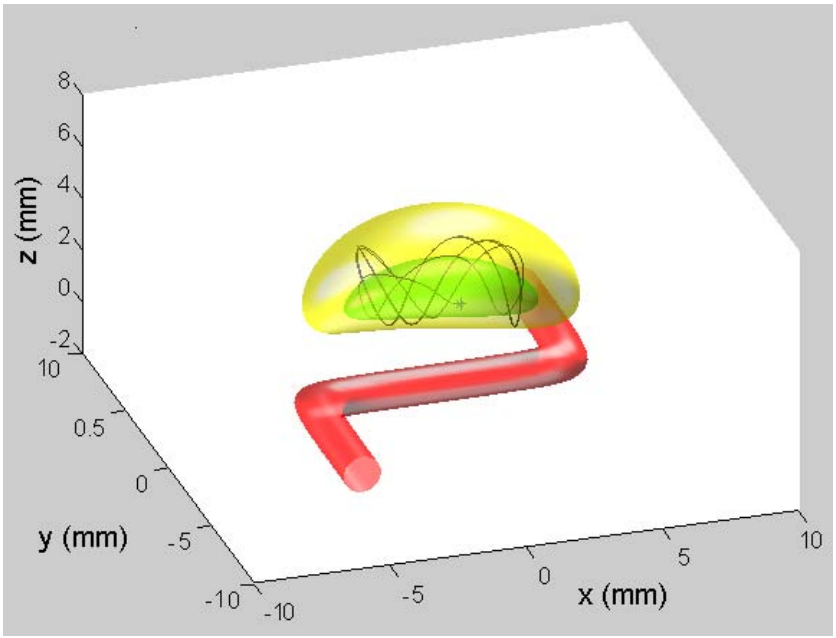

Figure 1.13: Simulated trajectory of an atom in the magnetic trap.

2 — QUANTUM NOISE IN EIT KERR SYSTEMS

The work discussed in this section was inspired by work discussing the giant Kerr nonlinearity created in EIT systems and a paper with the provocative title "Single-photon Kerr nonlinearities do not help quantum computation".[3]

Prior to this paper there were numerous papers discussing how a giant Kerr optical nonlinearity could be used to create two qubit gates (both CNOT and phase gates) for quantum computation, as trigger for quantum repeaters and quantum state regeneration, as quantum state preparation, and as photon number resolving detectors. It is only a slight exaggeration to say that it seemed like the Kerr nonlinearity was a cure all for everything except cancer (at least in the area of quantum measurement theory which is a pretty limited field). The only problem was that Kerr nonlinearities are extremely weak and require huge macroscopic fields with billions of photons to see a measurable effect. That was until the "giant" EIT-Kerr nonlinearity was discovered, and then it was speculated that the EIT-Kerr "scheme makes possible conditional phase shifts of the order of with single photons, which should be beneficial for quantum nondemolition measurements of weak signals and quantum logic gate operation."[4]

Even without considering quantum noise the early enthusiasm for EIT Kerr nonlinearities proved to be overly optimistic because EIT Kerr nonlinearities are as slow as they are large making the integrated signal to noise ratio for EIT Kerr QND measurements under normal conditions too small to achieve resolution of individual photons. However, combining the Kerr enhancement effects of an optical cavity and EIT it seemed possible to achieve single-photon QND measurements and all of the other benefits of giant Kerr nonlinearities. In earlier work we found that for the experimental configuration shown in Fig. 2.1, that the signal to noise ratio (SNR) for a QND measurement of photon number is

$$\frac{SNR}{n_S} \approx 10^{-2} \times Q\sqrt{\frac{N\sigma L}{k_0^2 A}} \ . \qquad (2.1)$$

In this measurement a signal beam and probe beam interact in an EIT Kerr medium (i.e. the atom cloud shaped as a red cigar in Fig 2.1), and the number of photons in the signal beam is imprinted on the probe beam (i.e. the EIT beam shown as blue elliptical beam in Fig. 2.1). By measuring the phase of the probe (EIT) beam using homodyne detection the number of signal photons is measured nondestructively and the signal field is projected into the measured number state. The large SNR given by Eq. 2.1 is largely due to the field enhancement of the optical cavity (i.e. the blue mirrors in Fig. 2.1), and the dipole trapping beams are to prevent the atom cloud from falling under the force of gravity. In Eq. (2.1) A is the signal field beam diameter, k_0 is the wavenumber (both signal and EIT fields are assumed to have approximately equal frequencies) , N the number density of atoms, σ is the absorption cross-section of the atoms, L is the length of the interaction region, and Q is the finesse of the signal cavity.

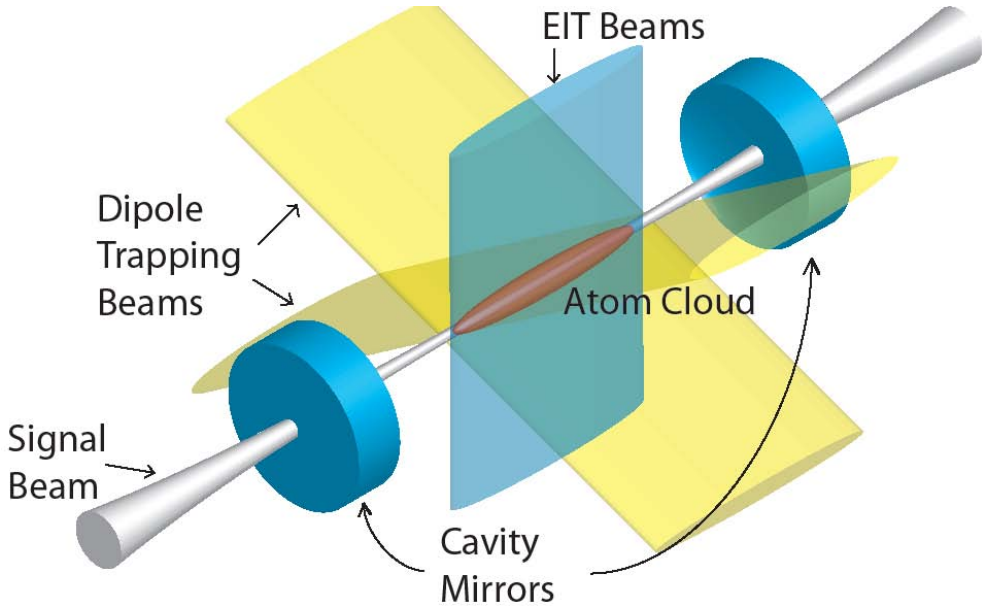

Figure 2.1: Diagram of an EIT Kerr experiment which could achieve large signal to noise ratio in the single photon limit. A signal field, which experiences a field enhancement due to propagating through a resonant optical cavity, creates cross-phase modulation an EIT beam via the EIT Kerr effect in a cold atomic cloud. The dipole trapping beams keep the atomic cloud from falling under the influence of gravity

The only problem with Eq. (2.1) is that it uses a semi-classical theory to determine the EIT Kerr nonlinearity, and thus does not account for vacuum fluctuations making the actually EIT Kerr phase shift noisy. It does however account for all other sources of quantum noise. There are reasons to believe that it is a good assumption to ignore this noise. To create a little more context for understanding this problem, consider that most EIT experiments use alkali atoms for their simplicity and good EIT characteristics. In this case noise in the EIT phase shift can only result from uncorrelated phase noise between the quantum states of two hyperfine magnetic sublevels, and this could only result from uncorrelated energy fluctuations between the two magnetic sublevels. However, the hyperfine splitting of the cesium (an alkali atom) ground state is used to define the second, and it is one of the most thoroughly measured values in all science. I have searched the literature and have not yet found where it discusses energy fluctuations in the ground states of cesium being an important noise source for determining the second. Also, EIT which is very sensitive to phase fluctuations in the ground states has been measured with line widths below 10 Hz in alkali atoms, and even in these cases the limiting factors seem to be decoherence due to buffer gas and wall collisions. Thus, it seemed reasonable to ignore the effects of vacuum fluctuations on the phase of the ground state. Although, I should point out that it is well known that vacuum fields do create an energy shift on the ground state which is known as the Lamb shift.

In Ref. [3] it is derived that when the commutation relation required by quantum mechanics are imposed on any Kerr nonlinearity, the fidelity of a two-qubit quantum gate derived from a Kerr nonlinearity must be poor. This is obviously because commutation relation imposes quantum noise on the Kerr nonlinearity. In contrast, Eq. (2.1) predicts that in theory the EIT Kerr nonlinearity can produce an arbitrarily good fidelity for a quantum gate. Therefore it

seems logical that there is important aspect of quantum noise that the derivation of Eq. (2.1) is ignoring, and that is the question we wish to resolve.

2.1 — The Lamb shift

It seems likely that the source of quantum noise responsible for reducing the fidelity of EIT Kerr measurements is also responsible for the Lamb shift, and thus our first effort at understanding this noise is to adapt calculations which predict the lamb shift. In particular we are adapting the calculation method employed by T. Welton.[5]The zero point fluctuations of the radiation field will effect the position of the electron causing it to spread out and experience a different smeared out Coulomb potential than if there were no noise associated with the quantum vacuum. In free space the non-relativistic equation of motion for an electron in an electric field is

$$m\ddot{x} = e\,\mathbf{E} \quad . \tag{2.1}$$

Given that the fluctuations about the mean value are defined by $\delta x \equiv x - \langle x \rangle$, the variance of the position is given by

$$\begin{aligned}
\left\langle (\delta x(t))^2 \right\rangle &= \int_{-\infty}^{\infty} \frac{d\omega}{2\pi} \int_{-\infty}^{\infty} \frac{d\omega'}{2\pi} \langle \delta x_\omega \, \delta x_{\omega'} \rangle \\
&= \int \frac{d\omega \, d\omega'}{(2\pi)^2} \frac{e^2}{m^2} \frac{1}{\omega^2 \omega'^2} \langle \mathbf{E}_\omega \mathbf{E}_{\omega'} \rangle \\
&= -\frac{e^2}{m^2} \left\langle \sum_{\mathbf{k},\lambda} \sum_{\mathbf{k}',\lambda'} \frac{\hbar 2\pi c k}{(ck)^2 (ck')^2} \left(a_{\mathbf{k},\lambda} - a^+_{\mathbf{k},\lambda} \right) \left(a_{\mathbf{k}',\lambda'} - a^+_{\mathbf{k}',\lambda'} \right) \right\rangle \qquad (2.2) \\
&= \frac{2e^2 \hbar}{\pi c^3 m^2} \int \frac{dk}{k},
\end{aligned}$$

where we have used the facts that the time-harmonic position fluctuations are

$$\delta x_\omega = -\frac{e}{m} \frac{\mathbf{E}_\omega}{\omega^2} \, , \tag{2.3}$$

and the quantized electric field is defined as

$$\mathbf{E}_\omega = i \sum_{\mathbf{k},\lambda} \sqrt{\frac{\hbar (2\pi)^3 ck}{V}} \left(a_{\mathbf{k},\lambda} \varepsilon_{\mathbf{k},\lambda} \delta(\omega - ck) - a^+_{\mathbf{k},\lambda} \varepsilon^*_{\mathbf{k},\lambda} \delta(\omega - ck) \right). \tag{2.4}$$

In order to evaluate Eq. (2.3) and achieve a none infinite result, physically realistic upper and lower limits need to be imposed on the integral over *k*. We will not review the arguments as to why the following limits are chosen, but upper and lower limits of $mc/\hbar$ and $Z\alpha\, mc/\hbar$ are the generally accepted limits.

It calculate the energy shift due to the zero point fluctuations we start with the Taylor expansion of the Coulomb potential

$$V\left(\langle \mathbf{x} \rangle + \delta \mathbf{x} \right) = V\left(\langle \mathbf{x} \rangle \right) + \delta x_i \nabla_i V + \frac{1}{2} + \delta x_i \delta x_j \nabla_i \nabla_j V + \ldots, \tag{2.5}$$

and use this to calculate the expectation value for the energy shift to first order

$$\left\langle V\left(\langle \mathbf{x}\rangle + \delta\,\mathbf{x}\right) - V\left(\langle \mathbf{x}\rangle\right)\right\rangle = \frac{1}{6}\left\langle (\delta\, x)^2 \right\rangle \int d\mathbf{x}\Psi_{n,l,m}\, \nabla^2 V\, \Psi^*_{n,l,m} \ . \tag{2.6}$$

For a Coulomb potential $V(r) = -4\pi Z\alpha\hbar c/r$, this simplifies to

$$\left\langle V\left(\langle \mathbf{x}\rangle + \delta\,\mathbf{x}\right) - V\left(\langle \mathbf{x}\rangle\right)\right\rangle = -\frac{4Z^4\alpha^5}{3\pi\, n^3} mc^2 \delta_{l,0} \log Z\alpha \ , \tag{2.7}$$

where we have used the fact that $\nabla^2(1/r) = -4\pi\delta(\mathbf{x})$.

2.2—Variance of the Lamb shift

To extend Welton's derivation of the Lamb shift to calculate the variance of the lamb shift we simply take the expectation value of the variance, which to first order is

$$\left\langle \left(V\left(\langle \mathbf{x}\rangle + \delta\,\mathbf{x}\right) - V\left(\langle \mathbf{x}\rangle\right)\right)^2 \right\rangle - \left\langle V\left(\langle \mathbf{x}\rangle + \delta\,\mathbf{x}\right) - V\left(\langle \mathbf{x}\rangle\right)\right\rangle^2 = \left\langle (\delta\, x)^2 \right\rangle \int \Psi_{n,l,m} (\nabla V)^2 \Psi^*_{n,l,m} \ . \tag{2.8}$$

Using Eq. (2.2) the facts that

$$(\nabla V)^2 = \frac{(4\pi\alpha\hbar c)^2}{r^4} \tag{2.9}$$

and

$$\begin{aligned} \int \left|\Psi_{n,l,m}\right|^2 \frac{1}{r^4} &= \int d\theta\, d\phi \sin\theta \left|Y_{l.m}(\theta,\phi)\right| \int dr \frac{\left|P_{n,l}{}^2\right|}{r^4} \\ &= \frac{Z^4\left[3n^2 - l(l+1)\right]}{2n^5(l+3/2)(l+1)(l+1/2)(l-1/2)} \end{aligned} \ , \tag{2.10}$$

we can calculate the variance given by Eq. (2.8). However, we are really interested in the variance of the phase which is the integral of the energy, and we have not yet performed this calculation. It is the variance of the phase which would also be of interest for time and frequency standards. Our study of the contribution of zero point fluctuations to the noise in EIT Kerr systems is still evolving, and this report is only an update on what has been completed.

References

[1] R. Long, T. Rom, W.Hansch, J. Reichel, “Long distance magnetic conveyor for precise positioning of ultracold atoms”, Eur. Phys. J. D **35** 125 (2005)
[2] P. Hommelhoff, W. Hansel, T. Steinmetz, T. W. Hansch, and J. Reichel, “Transporting, splitting and merging of atomic ensembles in a chip trap”, New J. Phys. **7**, 3 (2005)
[3] J. H. Shapiro, “Single-photon Kerr nonlinearities do not help quantum computation”, Phys. Rev. A **73**, 062305 (2006)
[4] H. Schmidt and A. Imamoglu, “Giant Kerr nonlinearies obtained by electromagnetically induced transparency”, Opt. Lett. **21**, 1936 (1996)
[5] T. A. Welton, “Some observable effects of the quantum-mechanical fluctuations of the electromagnetic field” Phys. Rev. **74**, 1157 (1948)

DISTRIBUTION

1	MS0123	D. Chavez, LDRD Office	1011
1	MS1082	K. Fortier	1725
1	MS1082	D. J. Armstrong	1725
1	MS1082	G. Biedermann	1725
1	MS1082	M. G. Blain	1725
1	MS1082	D. L. Stick	1725
1	MS1082	P. Schwindt	1725
1	MS1423	M. V. Pack	1128
1	MS1423	G. A. Hebner	1128
1	MS1421	J. A. Simmons	1120
1	MS1427	J. M. Phillips	1100
1	MS0899	Technical Library	9536 (electronic copy)